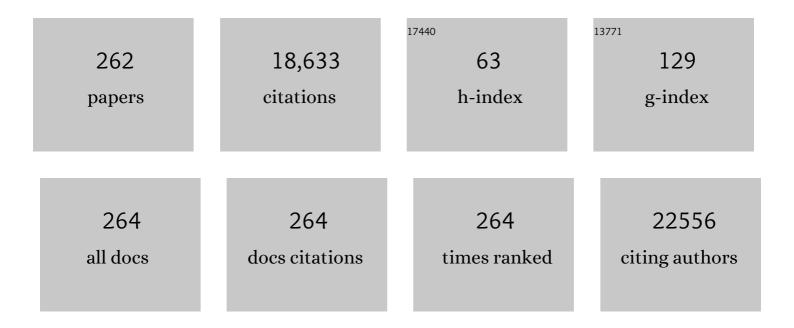
## Chih-Wei Chu

List of Publications by Year in descending order

Source: https://exaly.com/author-pdf/7650002/publications.pdf Version: 2024-02-01



#	Article	IF	CITATIONS
1	On the mechanism of conductivity enhancement in poly(3,4-ethylenedioxythiophene):poly(styrene) Tj ETQq1 1	0.784314	rgBT_/Qverlo
2	Epitaxial growth of a monolayer WSe <sub>2</sub> -MoS <sub>2</sub> lateral p-n junction with an atomically sharp interface. Science, 2015, 349, 524-528.	12.6	1,009
3	Transition metal oxides as the buffer layer for polymer photovoltaic cells. Applied Physics Letters, 2006, 88, 073508.	3.3	953
4	Programmable polymer thin film and non-volatile memory device. Nature Materials, 2004, 3, 918-922.	27.5	837
5	Efficient inverted polymer solar cells. Applied Physics Letters, 2006, 88, 253503.	3.3	743
6	Highly conductive PEDOT:PSS electrode by simple film treatment with methanol for ITO-free polymer solar cells. Energy and Environmental Science, 2012, 5, 9662.	30.8	705
7	Wafer-scale MoS2 thin layers prepared by MoO3 sulfurization. Nanoscale, 2012, 4, 6637.	5.6	621
8	Electrical Switching and Bistability in Organic/Polymeric Thin Films and Memory Devices. Advanced Functional Materials, 2006, 16, 1001-1014.	14.9	558
9	Organic Donor-Acceptor System Exhibiting Electrical Bistability for Use in Memory Devices. Advanced Materials, 2005, 17, 1440-1443.	21.0	396
10	High-performance organic thin-film transistors with metal oxide/metal bilayer electrode. Applied Physics Letters, 2005, 87, 193508.	3.3	338
11	Highly Conductive PEDOT:PSS Treated with Formic Acid for ITO-Free Polymer Solar Cells. ACS Applied Materials & Interfaces, 2014, 6, 2292-2299.	8.0	260
12	Effect of molecular weight of additives on the conductivity of PEDOT:PSS and efficiency for ITO-free organic solar cells. Journal of Materials Chemistry A, 2013, 1, 9907.	10.3	235
13	Opening an Electrical Band Gap of Bilayer Graphene with Molecular Doping. ACS Nano, 2011, 5, 7517-7524.	14.6	222
14	A Highly Stable Nonbiofouling Surface with Well-Packed Grafted Zwitterionic Polysulfobetaine for Plasma Protein Repulsion. Langmuir, 2008, 24, 5453-5458.	3.5	213
15	Organic thin-film transistors with nanocomposite dielectric gate insulator. Applied Physics Letters, 2004, 85, 3295-3297.	3.3	206
16	Surfactant-Free Water-Processable Photoconductive All-Carbon Composite. Journal of the American Chemical Society, 2011, 133, 4940-4947.	13.7	200
17	Layer-by-Layer Graphene/TCNQ Stacked Films as Conducting Anodes for Organic Solar Cells. ACS Nano, 2012, 6, 5031-5039.	14.6	199
18	Control of the nanoscale crystallinity and phase separation in polymer solar cells. Applied Physics Letters, 2008, 92, 103306.	3.3	196

#	Article	IF	CITATIONS
19	Enhanced Thermoelectric Performance of PEDOT:PSS Flexible Bulky Papers by Treatment with Secondary Dopants. ACS Applied Materials & Interfaces, 2015, 7, 94-100.	8.0	194
20	Synergistic improvements in stability and performance of lead iodide perovskite solar cells incorporating salt additives. Journal of Materials Chemistry A, 2016, 4, 1591-1597.	10.3	183
21	Photoluminescence Enhancement and Structure Repairing of Monolayer MoSe <sub>2</sub> by Hydrohalic Acid Treatment. ACS Nano, 2016, 10, 1454-1461.	14.6	179
22	Solution-processable antimony-based light-absorbing materials beyond lead halide perovskites. Journal of Materials Chemistry A, 2017, 5, 20843-20850.	10.3	169
23	Electric-field-induced charge transfer between gold nanoparticle and capping 2-naphthalenethiol and organic memory cells. Applied Physics Letters, 2005, 86, 123507.	3.3	153
24	Effective connecting architecture for tandem organic light-emitting devices. Applied Physics Letters, 2005, 87, 241121.	3.3	152
25	Effective Work Function Modulation of Graphene/Carbon Nanotube Composite Films As Transparent Cathodes for Organic Optoelectronics. ACS Nano, 2011, 5, 6262-6271.	14.6	150
26	Modified buffer layers for polymer photovoltaic devices. Applied Physics Letters, 2007, 90, 063509.	3.3	146
27	Hemocompatible Mixed-Charge Copolymer Brushes of Pseudozwitterionic Surfaces Resistant to Nonspecific Plasma Protein Fouling. Langmuir, 2010, 26, 3522-3530.	3.5	137
28	Photovoltaic Performance of Vapor-Assisted Solution-Processed Layer Polymorph of Cs <sub>3</sub> Sb <sub>2</sub> I <sub>9</sub> . ACS Applied Materials & Interfaces, 2018, 10, 2566-2573.	8.0	137
29	Planar Heterojunction Perovskite Solar Cells Incorporating Metal–Organic Framework Nanocrystals. Advanced Materials, 2015, 27, 7229-7235.	21.0	134
30	Tuning acceptor energy level for efficient charge collection in copper-phthalocyanine-based organic solar cells. Applied Physics Letters, 2006, 88, 153504.	3.3	132
31	Conducting polymer-based counter electrode for a quantum-dot-sensitized solar cell (QDSSC) with a polysulfide electrolyte. Electrochimica Acta, 2011, 57, 277-284.	5.2	128
32	Efficient photovoltaic energy conversion in tetracene-C60 based heterojunctions. Applied Physics Letters, 2005, 86, 243506.	3.3	124
33	Multiscale molecular simulations of the nanoscale morphologies of P3HT:PCBM blends for bulk heterojunction organic photovoltaic cells. Energy and Environmental Science, 2011, 4, 4124.	30.8	122
34	Improving the Light Trapping Efficiency of Plasmonic Polymer Solar Cells through Photon Management. Journal of Physical Chemistry C, 2012, 116, 20731-20737.	3.1	122
35	Dual-Thermoresponsive Phase Behavior of Blood Compatible Zwitterionic Copolymers Containing Nonionic Poly( <i>N</i> -isopropyl acrylamide). Biomacromolecules, 2009, 10, 2092-2100.	5.4	121
36	Efficient inverted solar cells using TiO <sub>2</sub> nanotube arrays. Nanotechnology, 2008, 19, 255202.	2.6	113

#	Article	IF	CITATIONS
37	Nucleation and crystal growth control for scalable solution-processed organic–inorganic hybrid perovskite solar cells. Journal of Materials Chemistry A, 2020, 8, 1578-1603.	10.3	112
38	A ternary cascade structure enhances the efficiency of polymer solar cells. Journal of Materials Chemistry, 2010, 20, 2820.	6.7	109
39	A high performance electrochemical sensor for acetaminophen based on a rGO–PEDOT nanotube composite modified electrode. Journal of Materials Chemistry A, 2014, 2, 7229-7237.	10.3	106
40	Gold nanoparticle-decorated graphene oxides for plasmonic-enhanced polymer photovoltaic devices. Nanoscale, 2014, 6, 1573-1579.	5.6	103
41	Converting Graphene Oxide Monolayers into Boron Carbonitride Nanosheets by Substitutional Doping. Small, 2012, 8, 1384-1391.	10.0	101
42	Tunable Novel Cyclopentadithiophene-Based Copolymers Containing Various Numbers of Bithiazole and Thienyl Units for Organic Photovoltaic Cell Applications. Macromolecules, 2009, 42, 3681-3693.	4.8	99
43	Organic Memory Device Fabricated Through Solution Processing. Proceedings of the IEEE, 2005, 93, 1287-1296.	21.3	98
44	Electrochemical characterization of the solvent-enhanced conductivity of poly(3,4-ethylenedioxythiophene) and its application in polymer solar cells. Journal of Materials Chemistry, 2009, 19, 3704.	6.7	95
45	Annealing effect of polymer bulk heterojunction solar cells based on polyfluorene and fullerene blend. Organic Electronics, 2009, 10, 27-33.	2.6	91
46	Solution-processed zinc oxide nanoparticles as interlayer materials for inverted organic solar cells. Solar Energy Materials and Solar Cells, 2013, 108, 156-163.	6.2	89
47	Towards solution processed all-carbon solar cells: a perspective. Energy and Environmental Science, 2012, 5, 7810.	30.8	87
48	Nanoparticle-induced negative differential resistance and memory effect in polymer bistable light-emitting device. Applied Physics Letters, 2006, 88, 123506.	3.3	86
49	Synthesis and applications of novel low bandgap star-burst molecules containing a triphenylamine core and dialkylated diketopyrrolopyrrole arms for organic photovoltaics. Journal of Materials Chemistry, 2012, 22, 7945.	6.7	86
50	Bifunctional separator as a polysulfide mediator for highly stable Li–S batteries. Journal of Materials Chemistry A, 2016, 4, 9661-9669.	10.3	86
51	Modified Separator Performing Dual Physical/Chemical Roles to Inhibit Polysulfide Shuttle Resulting in Ultrastable Li–S Batteries. ACS Nano, 2017, 11, 12436-12445.	14.6	83
52	Transparent and Flexible Inorganic Perovskite Photonic Artificial Synapses with Dualâ€Mode Operation. Advanced Functional Materials, 2021, 31, 2008259.	14.9	83
53	Using an Airbrush Pen for Layer-by-Layer Growth of Continuous Perovskite Thin Films for Hybrid Solar Cells. ACS Applied Materials & Interfaces, 2015, 7, 2359-2366.	8.0	82
54	Transparent electrodes based on conducting polymers for display applications. Displays, 2013, 34, 301-314.	3.7	78

#	Article	IF	CITATIONS
55	High quantity and quality few-layers transition metal disulfide nanosheets from wet-milling exfoliation. RSC Advances, 2013, 3, 13193.	3.6	76
56	Lead-Free Antimony-Based Light-Emitting Diodes through the Vapor–Anion-Exchange Method. ACS Applied Materials & Interfaces, 2019, 11, 35088-35094.	8.0	74
57	Efficiency Enhancement of Hybrid Perovskite Solar Cells with MEH-PPV Hole-Transporting Layers. Scientific Reports, 2016, 6, 34319.	3.3	72
58	Perovskite Quantum Dot Lasing in a Gap-Plasmon Nanocavity with Ultralow Threshold. ACS Nano, 2020, 14, 11670-11676.	14.6	71
59	2-Alkyl-5-thienyl-Substituted Benzo[1,2- <i>b</i> :4,5- <i>b</i> ′]dithiophene-Based Donor Molecules for Solution-Processed Organic Solar Cells. ACS Applied Materials & Interfaces, 2013, 5, 9494-9500.	8.0	70
60	Integration of organic light-emitting diode and organic transistor via a tandem structure. Applied Physics Letters, 2005, 86, 253503.	3.3	67
61	Synthesis and characterization of a narrowâ€bandgap polymer containing alternating cyclopentadithiophene and diketoâ€pyrroloâ€pyrrole units for solar cell applications. Journal of Polymer Science Part A, 2010, 48, 1669-1675.	2.3	67
62	Liquid Lenses and Driving Mechanisms: A Review. Journal of Adhesion Science and Technology, 2012, 26, 1773-1788.	2.6	67
63	Suppression of surface defects to achieve hysteresis-free inverted perovskite solar cells <i>via</i> quantum dot passivation. Journal of Materials Chemistry A, 2020, 8, 5263-5274.	10.3	67
64	Synthesis and applications of lowâ€bandgap conjugated polymers containing phenothiazine donor and various benzodiazole acceptors for polymer solar cells. Journal of Polymer Science Part A, 2010, 48, 4823-4834.	2.3	66
65	Polymer Optoelectronic Devices with Highâ€Conductivity Poly(3,4â€Ethylenedioxythiophene) Anodes. Journal of Macromolecular Science - Pure and Applied Chemistry, 2004, 41, 1497-1511.	2.2	65
66	Depth Profiling of Organic Films with X-ray Photoelectron Spectroscopy Using C60+and Ar+Co-Sputtering. Analytical Chemistry, 2008, 80, 3412-3415.	6.5	62
67	The Influence of Charge Trapping on the Electrochromic Performance of Poly(3,4-alkylenedioxythiophene) Derivatives. ACS Applied Materials & Interfaces, 2010, 2, 351-359.	8.0	62
68	Nanographite/polyaniline composite films as the counter electrodes for dye-sensitized solar cells. Journal of Materials Chemistry, 2011, 21, 10384.	6.7	62
69	Solutionâ€Processed Smallâ€Molecule Bulk Heterojunction Ambipolar Transistors. Advanced Functional Materials, 2014, 24, 2057-2063.	14.9	62
70	Complementary inverter circuits based on p-SnO2 and n-In2O3 thin film transistors. Applied Physics Letters, 2008, 92, .	3.3	61
71	rGO/SWCNT composites as novel electrode materials for electrochemical biosensing. Biosensors and Bioelectronics, 2013, 43, 173-179.	10.1	61
72	Flexible Fullerene Fieldâ€Effect Transistors Fabricated Through Solution Processing. Advanced Materials, 2009, 21, 4845-4849.	21.0	60

#	Article	IF	CITATIONS
73	Fabrication of multilayer organic solar cells through a stamping technique. Journal of Materials Chemistry, 2009, 19, 4077.	6.7	59
74	Solution-processable bismuth iodide nanosheets as hole transport layers for organic solar cells. Solar Energy Materials and Solar Cells, 2014, 121, 35-41.	6.2	59
75	Facile synthesis of composite tin oxide nanostructures for high-performance planar perovskite solar cells. Nano Energy, 2019, 60, 275-284.	16.0	57
76	Direct conversion of multilayer molybdenum trioxide to nanorods as multifunctional electrodes in lithium-ion batteries. Nanoscale, 2014, 6, 5484-5490.	5.6	55
77	Facile synthesis of carbon/MoO 3 nanocomposites as stable battery anodes. Journal of Power Sources, 2017, 348, 270-280.	7.8	54
78	Synthesis and characterization of novel lowâ€bandgap triphenylamineâ€based conjugated polymers with mainâ€chain donors and pendent acceptors for organic photovoltaics. Journal of Polymer Science Part A, 2010, 48, 5812-5823.	2.3	53
79	Hierarchical supramolecular hydrogels: self-assembly by peptides and photo-controlled release <i>via</i> host–guest interaction. Chemical Communications, 2017, 53, 12450-12453.	4.1	53
80	Realization of In2O3 thin film transistors through reactive evaporation process. Applied Physics Letters, 2007, 91, .	3.3	52
81	A Design Based on a Charge-Transfer Bilayer as an Electron Transport Layer for Improving the Performance and Stability in Planar Perovskite Solar Cells. Journal of Physical Chemistry C, 2018, 122, 236-244.	3.1	50
82	Anomalous p-channel amorphous oxide transistors based on tin oxide and their complementary circuits. Applied Physics Letters, 2008, 92, .	3.3	49
83	Dibenzo[f,h]thieno[3,4-b] quinoxaline-Based Small Molecules for Efficient Bulk-Heterojunction Solar Cells. Organic Letters, 2009, 11, 4898-4901.	4.6	49
84	Solvent-Annealing-Induced Self-Organization of Poly(3-hexylthiophene), a High-Performance Electrochromic Material. ACS Applied Materials & Interfaces, 2009, 1, 2821-2828.	8.0	49
85	Using a low temperature crystallization process to prepare anatase TiO2 buffer layers for air-stable inverted polymer solar cells. Energy and Environmental Science, 2010, 3, 654.	30.8	49
86	Plasma-assisted electrochemical exfoliation of graphite for rapid production of graphene sheets. RSC Advances, 2014, 4, 6946.	3.6	49
87	Bifacial Perovskite Solar Cells Featuring Semitransparent Electrodes. ACS Applied Materials & Interfaces, 2017, 9, 32635-32642.	8.0	49
88	Role of a hydrophobic scaffold in controlling the crystallization of methylammonium antimony iodide for efficient lead-free perovskite solar cells. Nano Energy, 2018, 45, 330-336.	16.0	49
89	Layered perovskite materials: key solutions for highly efficient and stable perovskite solar cells. Reports on Progress in Physics, 2020, 83, 086502.	20.1	48
90	Enhancement of tetracene photovoltaic devices with heat treatment. Applied Physics Letters, 2007, 90, 103501.	3.3	47

#	Article	IF	CITATIONS
91	Preparation of metal halide perovskite solar cells through a liquid droplet assisted method. Journal of Materials Chemistry A, 2015, 3, 9257-9263.	10.3	47
92	Manipulating location, polarity, and outgrowth length of neuron-like pheochromocytoma (PC-12) cells on patterned organic electrode arrays. Lab on A Chip, 2011, 11, 3674.	6.0	46
93	A counter electrode based on hollow spherical particles of polyaniline for a dye-sensitized solar cell. Journal of Materials Chemistry, 2012, 22, 14727.	6.7	46
94	Panchromatic heterojunction solar cells for Pb-free all-inorganic antimony based perovskite. Chemical Engineering Journal, 2021, 419, 129424.	12.7	46
95	Effects of nanomorphological changes on the performance of solar cells with blends of poly[9,9′-dioctyl-fluorene-co-bithiophene] and a soluble fullerene. Nanotechnology, 2009, 20, 025202.	2.6	45
96	Controlled mechanical cleavage of bulk niobium diselenide to nanoscaled sheet, rod, and particle structures for Pt-free dye-sensitized solar cells. Journal of Materials Chemistry A, 2014, 2, 11382-11390.	10.3	45
97	Efficient ternary bulk heterojunction solar cells based on small molecules only. Journal of Materials Chemistry A, 2015, 3, 10512-10518.	10.3	45
98	Solution-processed benzotrithiophene-based donor molecules for efficient bulk heterojunction solar cells. Journal of Materials Chemistry A, 2013, 1, 7767.	10.3	44
99	Lightâ€Responsive Arylazopyrazole Gelators: From Organic to Aqueous Media and from Supramolecular to Dynamic Covalent Chemistry. Chemistry - A European Journal, 2019, 25, 6131-6140.	3.3	44
100	Modulation of Donorâ´'Acceptor Interface through Thermal Treatment for Efficient Bilayer Organic Solar Cells. Journal of Physical Chemistry C, 2010, 114, 2764-2768.	3.1	43
101	Efficient bilayer polymer solar cells possessing planar mixed-heterojunction structures. Journal of Materials Chemistry, 2010, 20, 3295.	6.7	43
102	The investigation of donor-acceptor compatibility in bulk-heterojunction polymer systems. Applied Physics Letters, 2013, 103, .	3.3	43
103	New Helicene-Type Hole-Transporting Molecules for High-Performance and Durable Perovskite Solar Cells. ACS Applied Materials & Interfaces, 2018, 10, 41439-41449.	8.0	43
104	Balanced carrier transport in organic solar cells employing embedded indium-tin-oxide nanoelectrodes. Applied Physics Letters, 2011, 98, .	3.3	41
105	Synthesis and applications of 2,7â€carbazoleâ€based conjugated mainâ€chain copolymers containing electron deficient bithiazole units for organic solar cells. Journal of Polymer Science Part A, 2010, 48, 5479-5489.	2.3	40
106	Monitoring the 3D Nanostructures of Bulk Heterojunction Polymer Solar Cells Using Confocal Lifetime Imaging. Analytical Chemistry, 2010, 82, 1669-1673.	6.5	40
107	Synthesis and applications of main-chain Ru( <scp>ii</scp> ) metallo-polymers containing bis-terpyridyl ligands with various benzodiazole cores for solar cells. Journal of Materials Chemistry, 2011, 21, 1196-1205.	6.7	40
108	Synthesis and application of H-Bonded cross-linking polymers containing a conjugated pyridyl H-Acceptor side-chain polymer and various carbazole-based H-Donor dyes bearing symmetrical cyanoacrylic acids for organic solar cells. Polymer, 2010, 51, 6182-6192.	3.8	38

#	Article	IF	CITATIONS
109	Solution-processable electron transport layer for efficient hybrid perovskite solar cells beyond fullerenes. Solar Energy Materials and Solar Cells, 2017, 169, 78-85.	6.2	38
110	A lithium passivated MoO <sub>3</sub> nanobelt decorated polypropylene separator for fast-charging long-life Li–S batteries. Nanoscale, 2019, 11, 2892-2900.	5.6	38
111	Coral-like perovskite nanostructures for enhanced light-harvesting and accelerated charge extraction in perovskite solar cells. Nano Energy, 2019, 58, 138-146.	16.0	38
112	Achieving ambipolar vertical organic transistors via nanoscale interface modification. Applied Physics Letters, 2007, 91, 083507.	3.3	37
113	Dependence of channel thickness on the performance of In <sub>2</sub> O <sub>3</sub> thin film transistors. Journal Physics D: Applied Physics, 2008, 41, 092006.	2.8	37
114	Cost-effective dopant-free star-shaped oligo-aryl amines for high performance perovskite solar cells. Journal of Materials Chemistry A, 2019, 7, 14209-14221.	10.3	37
115	Organic single-crystal complementary inverter. Applied Physics Letters, 2006, 89, 222111.	3.3	36
116	Label-free detection of DNA using novel organic-based electrolyte-insulator-semiconductor. Biosensors and Bioelectronics, 2010, 25, 2706-2710.	10.1	35
117	Wet-milled transition metal oxide nanoparticles as buffer layers for bulk heterojunction solar cells. RSC Advances, 2012, 2, 7487.	3.6	35
118	High performance dye-sensitized solar cells based on platinum nanoparticle/multi-wall carbon nanotube counter electrodes: The role of annealing. Journal of Power Sources, 2012, 203, 274-281.	7.8	35
119	A novel ball milling technique for room temperature processing of TiO <sub>2</sub> nanoparticles employed as the electron transport layer in perovskite solar cells and modules. Journal of Materials Chemistry A, 2018, 6, 7114-7122.	10.3	35
120	Enhanced spectral response in polymer bulk heterojunction solar cells by using active materials with complementary spectra. Solar Energy Materials and Solar Cells, 2010, 94, 22-28.	6.2	34
121	Achieving efficient poly(3,4-ethylenedioxythiophene)-based supercapacitors by controlling the polymerization kinetics. Electrochimica Acta, 2011, 56, 7228-7234.	5.2	34
122	Influence of In doping on the thermoelectric properties of an AgSbTe2 compound with enhanced figure of merit. Journal of Materials Chemistry A, 2014, 2, 2839.	10.3	34
123	Efficient molecular solar cells processed from green solvent mixtures. Journal of Materials Chemistry A, 2017, 5, 571-582.	10.3	34
124	Recent Advances on Supramolecular Gels: From Stimuli-Responsive Gels to Co-Assembled and Self-Sorted Systems. Organic Materials, 2021, 03, 025-040.	2.0	34
125	Modulating Performance and Stability of Inorganic Lead-Free Perovskite Solar Cells via Lewis-Pair Mediation. ACS Applied Materials & Interfaces, 2020, 12, 32649-32657.	8.0	32
126	Bioinspired hole-conducting polymers for application in organic light-emitting diodes. Journal of Materials Chemistry, 2012, 22, 18127.	6.7	31

#	Article	IF	CITATIONS
127	Flexible Organic Thin Film Transistors Incorporating a Biodegradable CO2-Based Polymer as the Substrate and Dielectric Material. Scientific Reports, 2018, 8, 8146.	3.3	31
128	Top Illuminated Hysteresis-Free Perovskite Solar Cells Incorporating Microcavity Structures on Metal Electrodes: A Combined Experimental and Theoretical Approach. ACS Applied Materials & Interfaces, 2018, 10, 17973-17984.	8.0	31
129	Charge transporting enhancement of NiO photocathodes for p-type dye-sensitized solar cells. Electrochimica Acta, 2012, 66, 210-215.	5.2	30
130	High-Performance Organic Photovoltaics Incorporating an Active Layer with a Few Nanometer-Thick Third-Component Layer on a Binary Blend Layer. Nano Letters, 2021, 21, 2207-2215.	9.1	30
131	High-Performance Organic Solar Cells Featuring Double Bulk Heterojunction Structures with Vertical-Gradient Selenium Heterocyclic Nonfullerene Acceptor Concentrations. ACS Applied Materials & Interfaces, 2021, 13, 27227-27236.	8.0	30
132	Perovskite Quantum Wells Formation Mechanism for Stable Efficient Perovskite Photovoltaics—A Realâ€Time Phaseâ€Transition Study. Advanced Materials, 2021, 33, e2006238.	21.0	30
133	Correlation between Exciton Lifetime Distribution and Morphology of Bulk Heterojunction Films after Solvent Annealing. Journal of Physical Chemistry C, 2010, 114, 9062-9069.	3.1	29
134	Production of few-layer MoS <sub>2</sub> nanosheets through exfoliation of liquid N <sub>2</sub> –quenched bulk MoS <sub>2</sub> . RSC Advances, 2014, 4, 15586-15589.	3.6	29
135	Highly branched green phosphorescent tris-cyclometalated iridium(III) complexes for solution-processed organic light-emitting diodes. Organic Electronics, 2009, 10, 594-606.	2.6	27
136	New bioinspired hole injection/transport materials for highly efficient solution-processed phosphorescent organic light-emitting diodes. Nano Energy, 2015, 13, 1-8.	16.0	27
137	The 3 D Structure of Twisted Benzo[ghi]peryleneâ€Triimide Dimer as a Nonâ€Fullerene Acceptor for Inverted Perovskite Solar Cells. ChemSusChem, 2018, 11, 415-423.	6.8	27
138	Enhancement of photovoltaic properties in supramolecular polymer networks featuring a solar cell main-chain polymer H-bonded with conjugated cross-linkers. Polymer, 2012, 53, 1219-1228.	3.8	26
139	Organic solar cells featuring nanobowl structures. Energy and Environmental Science, 2013, 6, 1192.	30.8	26
140	Upconversion Plasmonic Lasing from an Organolead Trihalide Perovskite Nanocrystal with Low Threshold. ACS Photonics, 2021, 8, 335-342.	6.6	26
141	Facile Transfer Method for Fabricating Light-Harvesting Systems for Polymer Solar Cells. Journal of Physical Chemistry C, 2011, 115, 11864-11870.	3.1	25
142	Circular Dichroism Control of Tungsten Diselenide (WSe <sub>2</sub> ) Atomic Layers with Plasmonic Metamolecules. ACS Applied Materials & Interfaces, 2018, 10, 15996-16004.	8.0	25
143	Nanoscale Correlation between Exciton Dissociation and Carrier Transport in Silole-Containing Cyclopentadithiophene-Based Bulk Heterojunction Films. Journal of Physical Chemistry C, 2011, 115, 2398-2405.	3.1	24
144	Highly efficient organic–inorganic electroluminescence materials for solution-processed blue organic light-emitting diodes. Journal of Materials Chemistry C, 2016, 4, 6461-6465.	5.5	24

#	Article	lF	CITATIONS
145	Natural polymers for disposable organic thin film transistors. Organic Electronics, 2018, 54, 154-160.	2.6	24
146	Bilayer polymer solar cells prepared with transfer printing of active layers from controlled swelling/de-swelling of PDMS. Nano Energy, 2019, 63, 103826.	16.0	24
147	Controlled Growth of Nanofiber Network Hole Collection Layers with Pore Structure for Polymerâ^ Fullerene Solar Cells. Journal of Physical Chemistry C, 2008, 112, 19125-19130.	3.1	23
148	Molecular-weight-dependent nanoscale morphology in silole-containing cyclopentadithiophene polymer and fullerene derivative blends. Organic Electronics, 2011, 12, 1755-1762.	2.6	23
149	A new supramolecular film formed from a silsesquioxane derivative for application in proton exchange membranes. Journal of Materials Chemistry, 2012, 22, 731-734.	6.7	23
150	High-performance graphene/sulphur electrodes for flexible Li-ion batteries using the low-temperature spraying method. Nanoscale, 2015, 7, 8093-8100.	5.6	23
151	Toward environmentally compatible molecular solar cells processed from halogen-free solvents. Journal of Materials Chemistry A, 2016, 4, 7341-7351.	10.3	23
152	Modified Separators with Ultrathin Graphite Coating Simultaneously Mitigate the Issues of Metal Dendrites and Lithium Polysulfides to Provide Stable Lithium–Sulfur Batteries. ACS Sustainable Chemistry and Engineering, 2019, 7, 16604-16611.	6.7	23
153	Synthesis and characterization of a thiadiazole/benzoimidazoleâ€based copolymer for solar cell applications. Journal of Polymer Science Part A, 2010, 48, 4456-4464.	2.3	22
154	Efficiency enhancement of flexible organic light-emitting devices by using antireflection nanopillars. Optics Express, 2011, 19, A295.	3.4	22
155	The effect of solvent induced crystallinity of polymer layer on poly(3-hexylthiophene)/C70 bilayer solar cells. Solar Energy Materials and Solar Cells, 2011, 95, 419-422.	6.2	22
156	A dual-functional additive improves the performance of molecular bulk heterojunction photovoltaic cells. RSC Advances, 2014, 4, 9401.	3.6	22
157	Synergistic Effects of Morphological Control and Complementary Absorption in Efficient All-Small-Molecule Ternary-Blend Solar Cells. ACS Applied Materials & Interfaces, 2015, 7, 22542-22550.	8.0	22
158	Pentacene Thin-Film Transistor with PVP-Capped High-k MgO Dielectric Grown by Reactive Evaporation. Electrochemical and Solid-State Letters, 2008, 11, H118.	2.2	21
159	Three-Dimensional Nanoscale Imaging of Polymer Bulk-Heterojunction by Scanning Electrical Potential Microscopy and C <sub>60</sub> <sup>+</sup> Cluster Ion Slicing. Analytical Chemistry, 2009, 81, 8936-8941.	6.5	21
160	Flexible polymer solar cells prepared using hard stamps for the direct transfer printing of polymer blends with self-organized interfaces. Journal of Materials Chemistry, 2011, 21, 11378.	6.7	21
161	Highly Conductive PEDOT: PSS Electrode Treated with Polyethylene Glycol for ITO-Free Polymer Solar Cells. ECS Transactions, 2013, 58, 49-56.	0.5	21
162	Understanding and harnessing biomimetic molecular machines for NEMS actuation materials. IEEE Transactions on Automation Science and Engineering, 2006, 3, 254-259.	5.2	20

#	Article	IF	CITATIONS
163	A Strategic Buffer Layer of Polythiophene Enhances the Efficiency of Bulk Heterojunction Solar Cells. ACS Applied Materials & Interfaces, 2010, 2, 1281-1285.	8.0	20
164	Synthesis of Main hain Metallo opolymers Containing Donor and Acceptor Bisâ€Terpyridyl Ligands for Photovoltaic Applications. Macromolecular Rapid Communications, 2012, 33, 528-533.	3.9	20
165	Improved performance in n-channel organic thin film transistors by nanoscale interface modification. Organic Electronics, 2008, 9, 262-266.	2.6	19
166	Mitigating Metal Dendrite Formation in Lithium–Sulfur Batteries via Morphology-Tunable Graphene Oxide Interfaces. ACS Applied Materials & Interfaces, 2019, 11, 2060-2070.	8.0	19
167	Organic Base Modulation Triodes and Their Inverters on Flexible Substrates. Advanced Materials, 2009, 21, 1860-1864.	21.0	18
168	Nucleobase-grafted polycaprolactones as reversible networks in a novel biocompatible material. RSC Advances, 2013, 3, 12598.	3.6	18
169	UV- and NIR-Protective Semitransparent Smart Windows Based on Metal Halide Solar Cells. ACS Applied Energy Materials, 2018, 1, 632-637.	5.1	18
170	Synthesis, Photophysical Properties, and Fieldâ€Effect Characteristics of (Ethynylphenyl)benzimidazoleâ€Decorated Anthracene and Perylene Bisimide Derivatives. European Journal of Organic Chemistry, 2012, 2012, 2906-2915.	2.4	17
171	Graphene Nanosheets/Poly(3,4-ethylenedioxythiophene) Nanotubes Composite Materials for Electrochemical Biosensing Applications. Electrochimica Acta, 2015, 172, 61-70.	5.2	17
172	Pyrene-SH functionalized OTFT for detection of Hg2+ ions in aquatic environments. Organic Electronics, 2019, 69, 275-280.	2.6	17
173	Realization of ambipolar pentacene thin film transistors through dual interfacial engineering. Journal of Applied Physics, 2008, 103, 094519.	2.5	16
174	Supramolecular assembly of Hâ€bonded sideâ€chain polymers containing conjugated pyridyl Hâ€acceptor pendants and various lowâ€bandâ€gap Hâ€donor dyes bearing cyanoacrylic acid groups for organic solar cell applications. Journal of Polymer Science Part A, 2009, 47, 5998-6013.	2.3	16
175	New self-assembled supramolecular polymers formed by self-complementary sextuple hydrogen bond motifs. RSC Advances, 2012, 2, 9952.	3.6	16
176	Interfacial engineering affects the photocatalytic activity of poly(3-hexylthiophene)-modified TiO2. RSC Advances, 2013, 3, 26438.	3.6	16
177	Synthesis of fluorinated benzotriazole (BTZ)- and benzodithiophene (BDT)-based low-bandgap conjugated polymers for solar cell applications. Dyes and Pigments, 2017, 139, 349-360.	3.7	16
178	Efficient bulk heterjunction solar cells based on a low-bandgap polyfluorene copolymers and fullerene derivatives. Organic Electronics, 2009, 10, 1109-1115.	2.6	15
179	Performance of chromophore-type electrochromic devices employing indium tin oxide nanorod optical amplification. Solar Energy Materials and Solar Cells, 2012, 98, 191-197.	6.2	15
180	Modulation of work function of ITO by self-assembled monolayer and its effect on device characteristics of inverted perovskite solar cells. Organic Electronics, 2021, 98, 106297.	2.6	15

#	Article	IF	CITATIONS
181	Enhanced omnidirectional photon coupling via quasi-periodic patterning of indium-tin-oxide for organic thin-film solar cells. Organic Electronics, 2011, 12, 886-890.	2.6	14
182	Plasma electrolysis allows the facile and efficient production of graphite oxide from recycled graphite. RSC Advances, 2013, 3, 17402.	3.6	14
183	Stimuli-responsive polymer as gate dielectric for organic transistor sensors. Organic Electronics, 2020, 85, 105818.	2.6	14
184	Dual-color electrochromic films incorporating a periodic polymer nanostructure. RSC Advances, 2012, 2, 4746.	3.6	13
185	Synthesis of novel dithienothiophene―and 2,7â€carbazoleâ€based conjugated polymers and Hâ€bonded effects on electrochromic and photovoltaic properties. Journal of Polymer Science Part A, 2012, 50, 5011-5022.	2.3	13
186	Electrocatalytic SiC Nanoparticles/PEDOT:PSS Composite Thin Films as the Counter Electrodes of Dye‧ensitized Solar Cells. ChemElectroChem, 2014, 1, 1031-1039.	3.4	13
187	NbSe interlayers decrease interfacial recombination in Bil3-based hybrid solar cells. FlatChem, 2017, 5, 18-24.	5.6	13
188	Few-layer fluorine-functionalized graphene hole-selective contacts for efficient inverted perovskite solar cells. Chemical Engineering Journal, 2022, 430, 132831.	12.7	13
189	Balancing the ambipolar conduction for pentacene thin film transistors through bifunctional electrodes. Applied Physics Letters, 2008, 92, 253307.	3.3	12
190	Fine Tuning of HOMO Energy Levels for Low-Band-Gap Photovoltaic Copolymers Containing Cyclopentadithienopyrrole and Bithiazole Units. Macromolecular Chemistry and Physics, 2011, 212, 1960-1970.	2.2	12
191	Star Poly(N-isopropylacrylamide) Tethered to Polyhedral Oligomeric Silsesquioxane (POSS) Nanoparticles by a Combination of ATRP and Click Chemistry. Journal of Nanomaterials, 2012, 2012, 1-10.	2.7	12
192	Efficient reduction of graphene oxide catalyzed by copper. Physical Chemistry Chemical Physics, 2012, 14, 3083.	2.8	12
193	Novel metallo-dendrimers containing various Ru core ligands and dendritic thiophene arms for photovoltaic applications. Polymer Chemistry, 2014, 5, 5423-5435.	3.9	12
194	Enhanced Organic Solar Cell Performance by Lateral Side Chain Engineering on Benzodithiophene-Based Small Molecules. ACS Applied Energy Materials, 2018, 1, 3684-3692.	5.1	12
195	Dion–Jacobson Phase Perovskite Ca <sub>2</sub> Na <sub><i>n</i>–3</sub> Nb <sub><i>n</i></sub> O <sub>3<i>n</i>+1</sub> <sup>–(<i>n</i> = 4–6) Nanosheets as High-î<sup>®</sup> Photovoltaic Electrode Materials in a Solar Water-Splitting Cell. ACS Applied Nano Materials, 2020, 3, 6367-6375.</sup>	<b>5.</b> 0	12
196	Low-temperature processed bipolar metal oxide charge transporting layers for highly efficient perovskite solar cells. Solar Energy Materials and Solar Cells, 2021, 221, 110870.	6.2	12
197	Oxygen-Enriched α-MoO3– nanobelts suppress lithium dendrite formation in stable lithium-metal batteries. Journal of Power Sources, 2021, 507, 230306.	7.8	12
198	Dibenzo[f,h]thieno[3,4-b] quinoxaline–fullerene heterojunction bilayer solar cells with complementary spectrum coverage. Solar Energy Materials and Solar Cells, 2010, 94, 1767-1771.	6.2	11

#	Article	IF	CITATIONS
199	Introducing Postmetalation Metal–Organic Framework to Control Perovskite Crystal Growth for Efficient Perovskite Solar Cells. ACS Applied Materials & Interfaces, 2021, 13, 60125-60134.	8.0	11
200	Ambipolar transport behavior in In2O3/pentacene hybrid heterostructure and their complementary circuits. Applied Physics Letters, 2008, 93, .	3.3	10
201	Synthesis and applications of cyanoâ€vinyleneâ€based polymers containing cyclopentadithiophene and dithienosilole units for photovoltaic cells. Journal of Polymer Science Part A, 2011, 49, 3417-3425.	2.3	10
202	Improve efficiency of white organic light-emitting diodes by using nanosphere arrays in color conversion layers. Optics Express, 2012, 20, 3005.	3.4	10
203	Controlling vertical alignment of phthalocyanine nanofibers on transparent graphene-coated ITO electrodes for organic field emitters. Journal of Materials Chemistry, 2012, 22, 7837.	6.7	10
204	Star-shaped self-assembly of an organic thin film transistor sensor in the presence of Cu2+ and CNâ^' ions. Organic Electronics, 2014, 15, 582-589.	2.6	10
205	Enhance the light-harvesting capability of the ITO-free inverted small molecule solar cell by ZnO nanorods. Optics Express, 2016, 24, 17910.	3.4	10
206	Low-voltage complementary inverters employing organic vertical-type triodes. Organic Electronics, 2010, 11, 692-695.	2.6	9
207	Influence of molecular weight on silole-containing cyclopentadithiophene polymer and its impact on the electrochromic properties. Solar Energy Materials and Solar Cells, 2012, 98, 300-307.	6.2	9
208	Bioinspired assembly of functional block-copolymer nanotemplates. Soft Matter, 2013, 9, 9608.	2.7	9
209	Organic thin film transistors as selective sensing platforms for Hg2+ ions and the amino acidcysteine. Biosensors and Bioelectronics, 2013, 42, 76-79.	10.1	9
210	Complementary hydrogen bonding interaction-mediated hole injection in organic light-emitting devices. Journal of Materials Chemistry C, 2017, 5, 4736-4741.	5.5	9
211	Solution-Processed Perovskite/Perovskite Heterostructure Via a Grafting-Assisted Transfer Technique. ACS Applied Energy Materials, 2021, 4, 1962-1971.	5.1	9
212	Perspective on Predominant Metal Oxide Charge Transporting Materials for High-Performance Perovskite Solar Cells. Frontiers in Materials, 2021, 8, .	2.4	9
213	Using metal/organic junction engineering to prepare an efficient organic base-modulation triode and its inverter. Organic Electronics, 2009, 10, 1636-1640.	2.6	8
214	1-(3-Methoxycarbonyl)propyl-2-selenyl-[6,6]-methanofullerene as a n-Type Material for Organic Solar Cells. Synthetic Metals, 2011, 161, 1264-1269.	3.9	8
215	Applications of novel dithienothiophene- and 2,7-carbazole-based conjugated polymers with surface-modified ZnO nanoparticles for organic photovoltaic cells. Thin Solid Films, 2011, 519, 5212-5218.	1.8	8
216	Stable organic thin film transducers for biochemical and label-free sensing under physiological conditions. Journal of Materials Chemistry, 2012, 22, 16506.	6.7	8

#	Article	IF	CITATIONS
217	Efficiency enhancement of organic solar cells using peroxo-polytitanic acid coated silver nanowires as transparent electrodes. RSC Advances, 2015, 5, 18990-18996.	3.6	8
218	Quantitative Characterization and Mechanism of Formation of Multilength-scale Bulk Heterojunction Structures in Highly Efficient Solution-Processed Small-Molecule Organic Solar Cells. Journal of Physical Chemistry C, 2015, 119, 16507-16517.	3.1	8
219	Wetâ€milled anatase titanium oxide nanoparticles as a buffer layer for airâ€stable bulk heterojunction solar cells. Progress in Photovoltaics: Research and Applications, 2015, 23, 1017-1024.	8.1	8
220	Water-soluble fullerene-functionalized polymer micelles for efficient aqueous-processed conductive devices. Polymer Chemistry, 2017, 8, 7469-7474.	3.9	8
221	Asymmetric Benzotrithiophene-Based Hole Transporting Materials Provide High-Efficiency Perovskite Solar Cells. ACS Applied Materials & Interfaces, 2020, , .	8.0	8
222	Perfluorinated ionomer and poly(3,4-ethylenedioxythiophene) colloid as a hole transporting layer for optoelectronic devices. Journal of Materials Chemistry A, 2021, 9, 17967-17977.	10.3	8
223	Synthesis and applications of a novel supramolecular polymer network with multiple Hâ€bonded melamine pendants and uracil crosslinkers. Journal of Polymer Science Part A, 2012, 50, 967-975.	2.3	7
224	Study on Oxidation State Dependent Electrocatalytic Ability for I <sup>â^'</sup> /I <sub>3</sub> <sup>â^'</sup> Redox Reaction of Reduced Graphene Oxides. Electroanalysis, 2014, 26, 147-155.	2.9	7
225	Fabrication of flexible indium tin oxide-free polymer solar cells with silver nanowire transparent electrode. Japanese Journal of Applied Physics, 2018, 57, 03DD01.	1.5	7
226	Coreâ€Twisted Tetrachloroperylenediimides: Lowâ€Cost and Efficient Nonâ€Fullerene Organic Electronâ€Transporting Materials for Inverted Planar Perovskite Solar Cells. ChemSusChem, 2020, 13, 3686-3695.	6.8	7
227	Benzodithiophene-based small molecules with various termini as hole transporting materials in efficient planar perovskite solar cells. Organic Electronics, 2021, 89, 106010.	2.6	7
228	Sequential stacking of a thin BHJ layer acting as a morphology regulator for efficiency enhancement in non-fullerene ternary solar cells. Chemical Engineering Journal, 2022, 433, 134337.	12.7	7
229	In situ infrared spectroscopic studies of molecular behavior in nanoelectronic devices. , 0, , .		6
230	A cascade energy band structure enhances the carrier energy in organic vertical-type triodes. Organic Electronics, 2013, 14, 2284-2289.	2.6	6
231	Hybrid TiOx/fluoropolymer bi-layer dielectrics for low-voltage complementary inverters. Organic Electronics, 2010, 11, 154-158.	2.6	5
232	Reduced optical loss in mechanically stacked multi-junction organic solar cells exhibiting complementary absorptions. Optics Express, 2014, 22, A481.	3.4	5
233	Sweetening Lithium Metal Interface by High Surface and Adhesive Energy Coating of Crystalline αâ€≺scp>dâ€Glucose Film to Inhibit Dendrite Growth. Small, 2022, 18, .	10.0	5
234	Efficient organic optoelectronics with multilayer structures. Journal of Materials Chemistry, 2012, 22, 1364-1369.	6.7	4

#	Article	IF	CITATIONS
235	Optimization of polymer light emitting devices using TiOx electron transport layers and prism sheets. Organic Electronics, 2012, 13, 2667-2670.	2.6	4
236	Capillarityâ€Assisted Electrostatic Assembly of Hierarchically Functional 3D Graphene: TiO <sub>2</sub> Hybrid Photoanodes. Advanced Materials Interfaces, 2015, 2, 1500292.	3.7	4
237	Well-aligned Vertically Oriented ZnO Nanorod Arrays and their Application in Inverted Small Molecule Solar Cells. Journal of Visualized Experiments, 2018, , .	0.3	4
238	Improved conversion efficiency of perovskite solar cells converted from thermally deposited lead iodide with dimethyl sulfoxide-treated poly(3,4-ethylenedioxythiophene) poly(styrene sulfonate). Organic Electronics, 2019, 73, 266-272.	2.6	4
239	Long-lifespan lithium–metal batteries obtained using a perovskite intercalation layer to stabilize the lithium electrode. Journal of Materials Chemistry A, 2020, 8, 9137-9145.	10.3	4
240	Design of a Metal–Organic Frameworkâ€Đerived Co <sub>9</sub> S <sub>8</sub> /S Material for Achieving High Durability and High Performance of Lithium–Sulfur Batteries. ChemElectroChem, 2021, 8, 3040-3048.	3.4	4
241	Electrochemical Performance of Orthorhombic CsPbI3 Perovskite in Li-Ion Batteries. Materials, 2021, 14, 5718.	2.9	4
242	Enhancing the Areal Capacity and Stability of Cu <sub>2</sub> ZnSnS <sub>4</sub> Anode Materials by Carbon Coating: Mechanistic and Structural Studies During Lithiation and Delithiation. ACS Omega, 2022, 7, 9152-9163.	3.5	4
243	An amino-phthalocyanine additive enhances the efficiency of perovskite solar cells through defect passivation in mixed-halide films. Organic Electronics, 2022, 108, 106568.	2.6	4
244	Ubiquitous carrier harvesting in organic solar cells with embedded indium–tin-oxide nano-electrodes. Solar Energy Materials and Solar Cells, 2013, 118, 102-108.	6.2	3
245	Ultrafast dynamics of quasiparticles and coherent acoustic phonons in slightly underdoped (BaK)Fe2As2. Scientific Reports, 2016, 6, 25962.	3.3	3
246	Microstructural intra-granular cracking in Cu <sub>2</sub> ZnSnS <sub>4</sub> @C thin-film anode enhanced the electrochemical performance in lithium-ion battery applications. Materials Advances, 2021, 2, 5672-5685.	5.4	3
247	Discrete Metal-Oxide Clusters with Organofunctionalization as High-Performance Anode Materials. ACS Applied Energy Materials, 2021, 4, 643-654.	5.1	3
248	Flexible Indium Tin Oxide-Free Polymer Solar Cells with Silver Nanowire Electrodes. Journal of Nanoelectronics and Optoelectronics, 2017, 12, 839-843.	0.5	3
249	Core-twisted tetrachloroperylenediimide additives improve the crystallinity of perovskites to provide efficient perovskite solar cells. Solar Energy Materials and Solar Cells, 2022, 243, 111779.	6.2	3
250	Efficient and stable polymer solar cells prepared using plasmonic graphene oxides as anode buffers. Semiconductor Science and Technology, 2015, 30, 085013.	2.0	2
251	Pâ€117: High Efficient Color Conversion Layers for White Organic Lightâ€Emitting Diodes using Polystyrene Nanosphere Monolayers. Digest of Technical Papers SID International Symposium, 2012, 43, 1499-1502.	0.3	1
252	Photoanodes: Capillarityâ€Assisted Electrostatic Assembly of Hierarchically Functional 3D Graphene: TiO <sub>2</sub> Hybrid Photoanodes (Adv. Mater. Interfaces 17/2015). Advanced Materials Interfaces, 2015, 2, .	3.7	1

#	Article	IF	CITATIONS
253	Polymer electrical bistable device and memory cells. Materials Research Society Symposia Proceedings, 2004, 830, 323.	0.1	0
254	The Mechanism and Effective Connecting Structure for Tandem Organic Light-Emitting Devices. , 0, , .		0
255	Balanced carrier transport in organic solar cells using implanted indium-tin-oxide nano-columns. , 2011, , .		0
256	Pâ€179: Efficiency Enhancement of PLED by Using TiO <sub>x</sub> Electron Transport Layer with Prism Sheet Attachment. Digest of Technical Papers SID International Symposium, 2011, 42, 1770-1772.	0.3	0
257	Pâ€113: Efficiency and Image Enhancement of Flexible Organic Lightâ€Emitting Devices by Using Antireflection Nanopillars. Digest of Technical Papers SID International Symposium, 2011, 42, 1531-1534.	0.3	0
258	All-Carbon Composite for Photovoltaics. Materials Research Society Symposia Proceedings, 2011, 1344, 1.	0.1	0
259	Electrocatalytic SiC Nanoparticles/PEDOT:PSS Composite Thin Films as the Counter Electrodes of Dye-Sensitized Solar Cells. ChemElectroChem, 2014, 1, 961-961.	3.4	0
260	ITO-free inverted small molecule solar cells. , 2016, , .		0
261	A Superficial new Solid-State Synthesis of SnO2 for High-Performance and Stable Perovskite Solar Cells. , 0, , .		0
262	(Digital Presentation) Stable Passivation Layer of Oxygen Deficient α-MoO <sub>3-X</sub> Nanobelts Suppress Li Dendrites to Achieve High-Capacity Li-S Battery. ECS Meeting Abstracts, 2022, MA2022-01, 517-517.	0.0	0